Pergamon

Tetrahedron 57 (2001) 2991–2996

TETRAHEDRON

Aromatic interactions in the synthesis and conformation of two collapsible tetracationic cyclophanes

Milind D. Sindkhedkar, Hormuzd R. Mulla, Mark A. Wurth and Arthur Cammers-Goodwin*

Department of Chemistry, University of Kentucky, Lexington KY 40506-0055, USA

Received 20 December 2000; accepted 2 February 2001

Abstract—The conformations of tetracationic paracyclophane and metacyclophane derivatives containing quaternary salts of *para*-2,2-diazaterphenyl were investigated. The molecules were synthesized as the bromide and hexafluorophosphate salts which allowed solubility in aqueous and organic solvents. Molecular mechanics led to the notion that these cyclophanes would populate collapsed and open conformations in water and only populate open conformers in organic solvent. VT NMR studies indicated that the open and the collapsed conformers did not exchange on the NMR timescale. Large, positively charged clefts in one of these conformers bound flat anions between pyridinium rings as would molecular-scale tweezers. © 2001 Elsevier Science Ltd. All rights reserved.

1. Introduction

Conformational analyses of derivatives of *N*-benzyl-2-phenylpyridinium[1,2] **1** have demonstrated that these molecules are good solution phase models for face-to-face, π-stacking in many pure solvents and mixed aqueous solvents.[1–4] In Fig. 1, cation **1** is a structural component of tetracationic cyclophanes **2**·4Br$^-$ and **3**·4Br$^-$, [1.1.1.1](*N,N′,N″,N′″*)*para*-2,2″-diazaterphenylparacyclophanium bromide and [1.1.1.1](*N,N′,N″,N′″*)*para*-2,2″-diazaterphenylmetacyclophanium bromide, respectively.[5] Calculations showed that **1** and **2** could exist as opened or collapsed conformers. The collapsed conformers maximized interactions between aromatic hydrocarbons surface area. Calculations also indicated that cyclophanes **2** and **3** should have collapsed (caricaturized in Fig. 1) and stacked the all-carbon aromatic rings face-to-face in structures that resembled the lowest-energy conformers of non-macrocyclic derivatives of **1**. This result bore some similarity to a previous study in which cyclophanes served as templates for edge-to-face interactions.[6] In the current study, we report the synthesis of the bromide and hexafluorophosphate salts of **2** and **3** and propose that similarity between the conformational preferences of **1a–g** (solid state X-ray, solution phase ^{1}H NMR and calculations with MM2*) and the calculated, lowest-energy, conformers of cyclophanes **2** and **3** (MM2*, Amber*, OPLS) rationalizes facile cyclization to the cyclophanes.[7] Even though metals and charged organic guests have been reported to serve as templates for macrocyclization of polyethers,[8,9] carceplexes,[10,11] and catenanes,[12–14] the propensity of aromatic rings to stack is a weak intermolecular force that is rarely cited as the sole component in the control of organic syntheses. Much work has been done in the last 10 years involving cyclophane derivatives of pyridinium salts.[15,16] This investigation

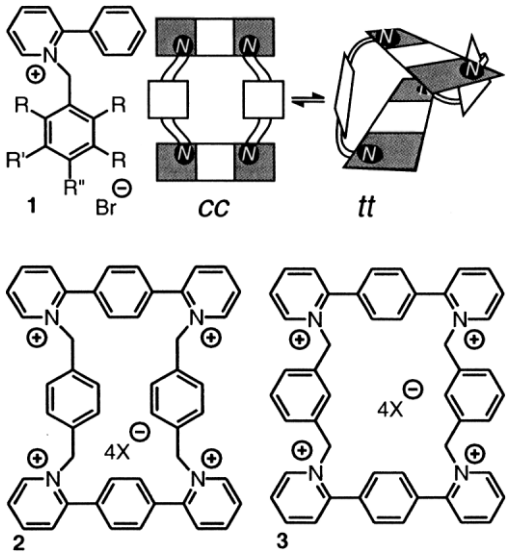

Figure 1. Structural similarities between **1** and macrocyclic **2** and **3** translated to similar conformational preferences. X-Ray crystal structures of **1a–g** were reported previously. Despite repeated attempts, diffraction quality crystals of **2** and **3** were not obtained. **1a**: R,R′,R″=H; **1b**: R″=OMe, R,R′=H; **1c**: R″=CN, R,R′=H; **1d**: R^2=CF$_3$, R,R′=H; **1e**: R^2=CF$_3$, R,R′=F; **1f**: R,R′=H, R^2=CH$_2$-*N*-2-phenylpyridinium; **1g**: R,R^2=H, R′=CH$_2$-*N*-2-phenylpyridinium. The collapse of **2** and **3** is caricaturized at the bottom of the figure. Note that the *N* atoms of the diazaterphenyl units are both *syn* or *cis* to one another in the **cc** conformer and *anti* or *trans* in the **tt** conformer.

Keywords: π-stacking; cyclophane; solvation; molecular mechanics; GB/SA; conformation; molecular recognition; anion binding; molecular tweezers; dynamic NMR.

* Corresponding author. Tel.: +1-859-323-8977; fax: +1-859-323-1069; e-mail: acgood1@pop.uky.edu

0040–4020/01/$ - see front matter
PII: S0040-4020(01)00162-4

of the conformations of **2** and **3** contributes to knowledge of molecular recognition events and conformational preferences of related cationic cyclophanes. Cyclophanes **2** and **3** were big enough to afford both expanded and collapsed conformers, yet these macrocycles were small enough for differences in strain between *para* **2** and *meta* **3** to have been manifest in their folding.

2. Results and discussion

Interest in conformational control in molecules that can intramolecularly stack aromatic rings under a variety of conditions led to the investigation of cyclophane derivatives of **1** and inspired inclusion of *p* and *m*-2,2″-azaterphenyl **4**[17] and **5**[18] in synthetic schemes. Efficient syntheses of **4** and **5** based on Suzuki coupling were developed; see Section 6. *Bis*-pyridine **5** did not cyclize efficiently when treated with 1,3- or 1,4-dibromoxylene. However, substitution processes in the reaction of **4** and 1,3- or 1,4-dibromoxylene led to efficient cyclization to **2** and **3** supposedly from the dimerization of **6** and **7**. By adding 1,3-dibromoxylene in greater than stoichiometric amounts, **8** and **9** could be isolated. However, cyclization to **2** competed in the reaction of excess 1,4-dibromoxylene with **4**. From heated solutions of DMF containing 1:1 mixtures of 1,3- or 1,4-dibromoxylene and **4**, cyclophanes **2** or **3** precipitated in ca. 80% yield (Fig. 2).

3. Cyclophane conformation

The MM2 force field successfully assessed conformational preferences of charged cyclophane derivatives.[19] Also molecular mechanics using Amber and OPLS have been applied towards the conformation of cyclophanes rich in heteroatoms.[16] Molecular modeling of **2** and **3** (MM2*, Amber* and OPLS)[20] indicated that strain ($E_{stretching}+E_{bending}+E_{torsional}$) destabilized **2** less than **3** ($1.2–8.4$ kJ mol^{-1}, with all three force fields, with $CHCl_3$ and water GB/SA continua[21] as computational solvent models). Five out of six calculations reported decreased electrostatic repulsion ($15–56$ kJ mol^{-1}) in **2** versus **3**. The relative stability of **2** paralleled these calculations since decomposition of **3**·4Br$^-$ occurred within a week at room temperature whereas **2**·4Br$^-$ was notably more stable. However as the PF_6^- salts, **2** and **3** were stable indefinitely at room temperature.[22]

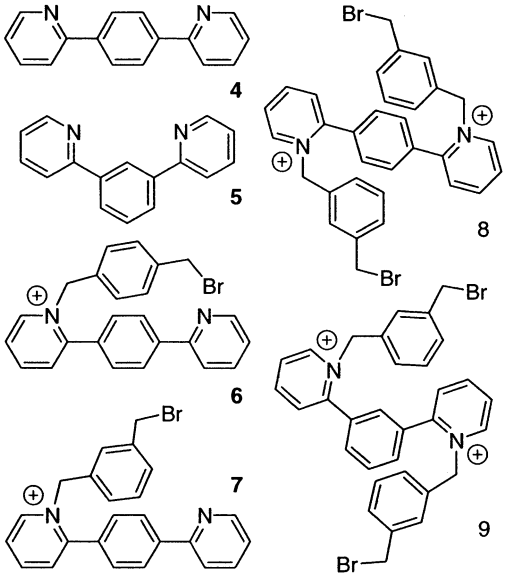

Figure 2. *para* and *meta*-2,2″-Diazaterphenyl **4** and **5**. Monoadducts **6** and **7** supposedly dimerized to form **2** and **3**. Dications **8** and **9** were obtained in reactions of **4** or **5** and excess 1,3-dibromoxylene.

Monte Carlo sampling of the conformational space of **3** with Amber*, OPLS and MM2* generated three sets of conformers. The nitrogen atom in the pyridinium rings of the *p*-2,2″-diazaterphenyl subunit could either be *trans* or *cis* to one another (see the cartoon in Fig. 1) and there were two of these subunits, thus the conformers are herein denoted **tt**, **cc**, or **tc** (not shown) in Figs. 4–7. Ring strain edited conformer **3tc** out of the conformational distribution of **3**. Even though conformer **2tc** was energetically accessible it was calculated to be higher in energy than **2tt** and **2cc**.

Calculated conformers **2tt** and **3tt** resembled the calculated minimum-energy conformers and the experimental solid-state of derivatives of **1a–g** reported previously.[2,3] Cation **1** promotes face-to-face, center-to-edge π-stacking (FFCE, see Fig. 3) not FFCC or EF π-stacking due to the torsional strain in the corresponding conformers of **1**. Similarity between low-energy conformers of **1** and those of **2** and **3** predicted that **2** and **3** would collapse to optimize interactions between aromatic rings despite possible electrostatic repulsion in these cyclophanes. Furthermore, contacts between the neutral aromatic moieties were predicted in the lowest-energy conformers of **2** and **3**, due to electrostatic repulsion between the charged rings. A similar argument was given for electrostatic conformational control in *bis*-pyridinium derivatives **1f** and **1g**.[3,4] An inverse relationship between the azabiphenyl dihedral angle (N1C2C7C8 in Fig. 3) and the *N*-benzyl dihedral angle (C2N1C13C14) optimized π-stacking in derivatives of **1**. Dihedral angles in the calculated low-energy conformer of **3tt** (MM2*, water GB/SA) exemplified this inverse relationship between the azabiphenyl dihedral angle (85.8 and 78.1°) and the *N*-benzyl dihedral angle (54.6 and 52.2°). Analogous dihedral angles in the less strained cyclophane **2** and in the ring strain-free derivatives of **1** had *smaller* azabiphenyl dihedral angles and *larger N*-benzyl dihedral angles. The all-carbon rings in nine out of ten X-ray crystal structures of derivatives of **1** were FFCE π-stacked. The average *N*-benzyl dihedral angle and the average azabiphenyl

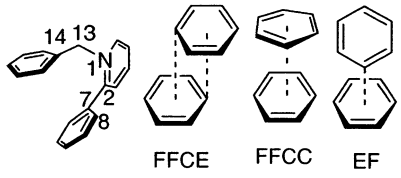

Figure 3. In derivatives of **1**, as the *N*-benzyl dihedral angle (C2N1C13C14) decreases, the 2-azabiphenyl dihedral angle (N1C2C7C8) approaches 90° for optimal π-stacking allowing one aromatic ring to slide above the other. This relationship is only true while torsional strain in **1** remains low. Also shown are the spatial relationships between two C_6H_6 molecules denoted by FFCE, FFCC and EF stacking motifs (F=face, C=center, E=edge).

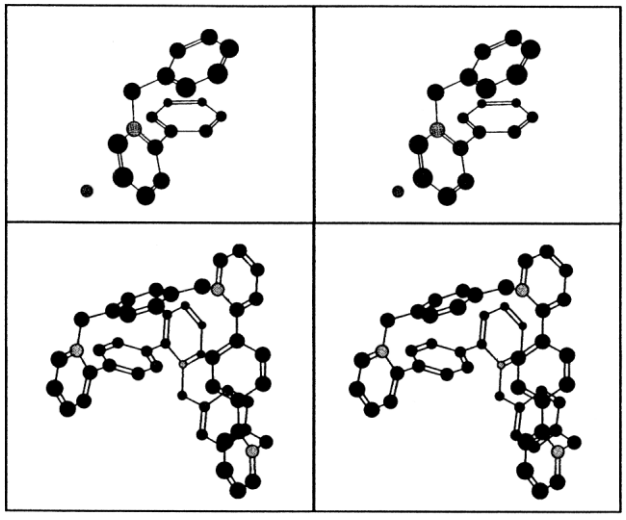

Figure 4. These stereo structures show conformational similarities between the solid state of **1a** and the low-energy conformation, **2tt**, minimized with MM2* and GB/SA water. The analogous stacked conformational substructure of **1a** in **2tt** is visible to the left and to the lower right in the cyclophane in the figure. The sphere in the X-ray structure of **1a** is a bromide anion. Transannular pairs of pyridinium rings are at unequal distances in **2tt**. The proximal pair (7 Å, N-to-N) appears toward the upper right of the structure and the remote pair (9.4 Å, N-to-N) is at the bottom of the structure.

dihedral angle in these crystalline derivatives of **1** were 64.5±7 and 65.4±6° respectively. Analogous calculated dihedral angles (MM2* GB/SA water) in **2tt** for the *N*-benzyl dihedral angle (63.6 and 61.7°) and 2-azabiphenyl dihedral angle (66.1 and 71.4°) were within the standard deviation of the averages of the dihedral angles found in the solid-states of acyclic **1a**–**g**.

Recurring conformational patterns between derivatives of **1**; and **2**, and **3** were observed. These can be seen in Figs. 4 and 5 in which the MM2*, lowest energy conformers **2tt** and **3tt**

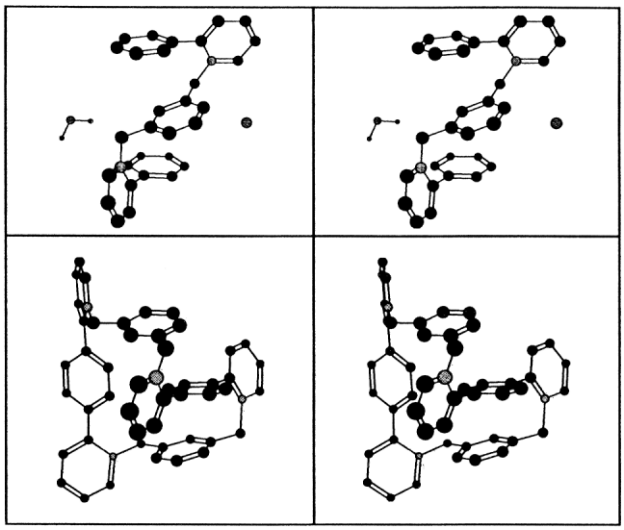

Figure 5. Analogous conformation was found in the solid state of **1g** and the MM2* predicted lowest-energy conformer, **3tt**. Both molecules possessed three rings π-stacked in an FFCE manner. Dication **1g** cocrystallizes[3] with one water molecule, which appears in the figure along with a bromide anion.

are structurally compared to the solid states of **1a** and **1g**, respectively.

There was general agreement between the force fields regarding the relative stabilities of the conformers of **2** and **3**. Conformers **2tt** and **3tt** (Figs. 4 and 5) minimized energy in **2** and **3** when optimizations were performed with GB/SA water because the high dielectric field allowed intramolecular positive charges to come together without stark destabilization from electrostatic repulsion. Conformers **2cc** and **3cc** (Figs. 6 and 7) were also more compact when minimized in GB/SA water than the **cc** conformers minimized in GB/SA $CHCl_3$ due to electrostatic effects. Fig. 8 compares the force field-dependent, relative energies of the **tt**, **cc**, and **tc** families of conformers in GB/SA water and GB/SA

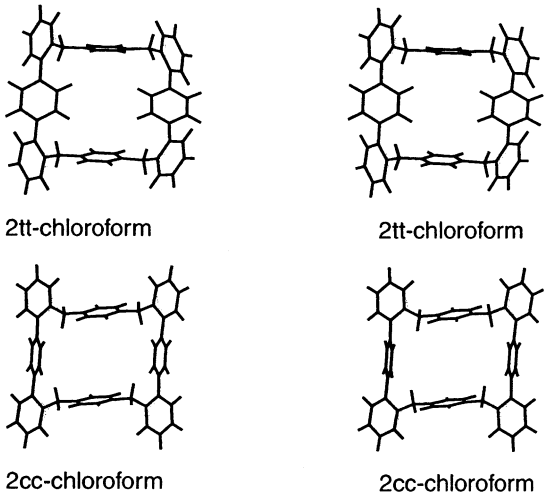

Figure 6. Stereodiagrams of calculated MM2* minima of **2** in continuum fields of water and chloroform. Calculations with Amber* and OPLS yielded analogous conformers.

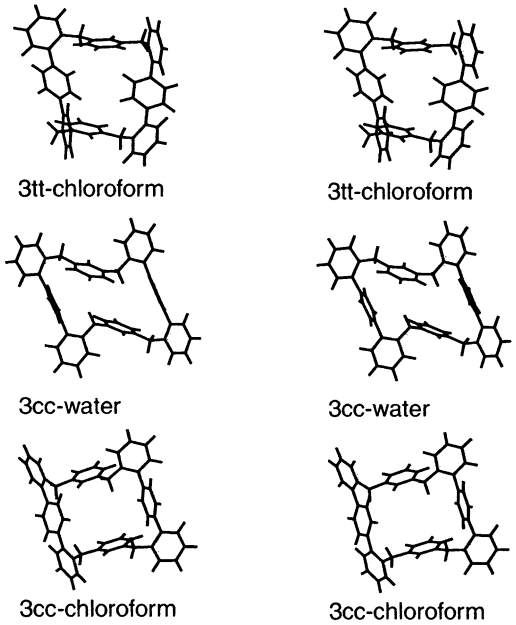

Figure 7. Stereodiagrams of calculated MM2* energy minima of **3** in continuum fields of water and chloroform. Calculations with Amber* and OPLS yielded analogous conformers.

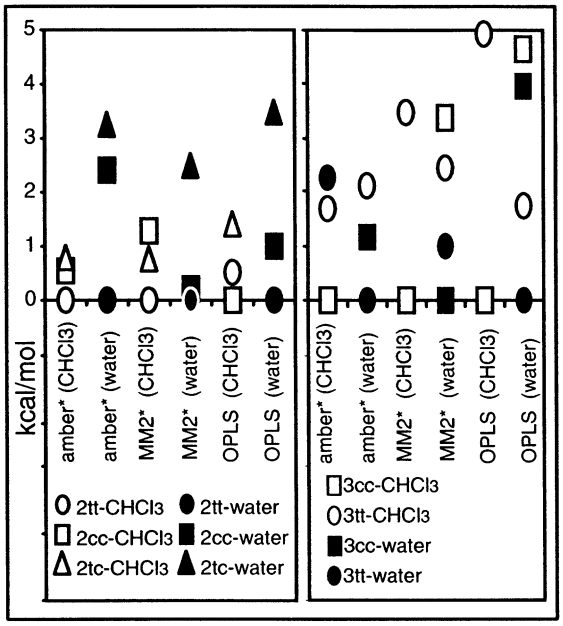

Figure 8. The relative energies in kcal mol^{-1} were referenced to the lowest energy conformer for each force field/solvent combination. To evaluate the solvent effect, the energies of the conformers minimized in GB/SA water (white icons) were calculated in GB/SA $CHCl_3$ without energy minimization, likewise. the low-energy conformers minimized in GB/SA $CHCl_3$ (black icons) were evaluated in water. Water obviously favored the compact **tt** conformer (except with cyclophane **3** using MM2*), whereas the favored conformers in $CHCl_3$ were **2tt** and **3cc**. Experimentally **tt**, **cc** and **tc** conformers might compete in solution because they differed by approximately 1 kcal mol^{-1} or less and the calculations did not account for ion pairing, or explicit solvent/solute interactions.

$CHCl_3$. To gauge the effect of solvation on the calculations, the energies of the lowest-energy conformers **2tt**, **2cc** and **2tc** minimized in GB/SA $CHCl_3$ were evaluated in GB/SA water without energy minimization. The results from these calculations also appear in Fig. 8 and suggest that GB/SA solvation drove conformational changes in cyclophane **2** ca. 2 kcal mol^{-1}. When structures minimized in GB/SA water were evaluated without minimization in GB/SA $CHCl_3$ the energies of these structures were high due to the inability of the low dielectric continuum to screen electrostatic interactions.

4. VT NMR

Attempts to conformationally characterize **2** or **3** further by ^{1}H VT NMR were frustrated by temperature invariant spectra. There are four possible reasons for temperature invariance. (1) The molecules may have been conformationally mobile at temperatures as low as −70°C. Solubility and solvent freezing limited the temperature range of VT NMR to ca. −70°C. Facile conformational mobility has been postulated previously for temperature invariance in ^{1}H NMR spectra of structurally similar, neutral cyclophanes.[23] However, line broadening in ^{1}H NMR spectra as a result of decreased rotation of CH_2–Ph bonds was evident at low temperature. Conformational changes like **tt→cc** would likely precede the rotation of CH_2–Ph bonds. (2) A second cause of temperature invariant NMR spectra could have been similar enthalpic stabilities of the **tt** and **cc** conformers. In this case the conformational equilibria would have shifted only slightly with temperature. Molecular mechanics predicted a 2 kcal mol^{-1} gradient between the **tt** and **cc** conformers of both **2** and **3**. This is within the range of accuracy of the calculation, given that the counter ions and explicit solvent molecules were not included. (3) Conformers **tt**, **cc** and **tc** may have had similar chemical shifts. This condition would have completely removed temperature dependence from the NMR signals. However diamagnetic anisotropy should have given rise to different chemical shifts between the compact **tt** conformer and the less compact **cc** conformer in **2** and **3** because the **tt** conformer held the aromatic rings closer together than the **cc** conformer. In the **tt** conformers the all-carbon rings were FFCE π-stacked and in **cc** these rings were splayed. (4) The most likely hypothesis for temperature invariance of the NMR spectra is that the **tt** and **cc** conformers did not exchange on the NMR timescale.

Locked **tt** and **cc** conformers were deduced from the following facts. There were small sharp signals in the ^{1}H NMR spectrum of **3** despite multiple purification attempts, suggestive that more than one conformer might have been populated at room temperature. In both ^{1}H and ^{13}C NMR spectra of the bromide salts of **2** there were indications of two spectrally analogous materials. Fig. 9 compares the ^{1}H NMR spectra of the **2**·4Br^- and **2**·4PF_6^- in D_2O and DMF-d_4, respectively. One component in samples of **2** was fluxional on the NMR timescale and could be partially removed from the mixture by repeated precipitations. The samples of **2** (and **3**) that contained these extra materials analyzed well by elemental analysis and did not have any residual RCH_2Br or RCH_2OH signals expected if cyclization were incomplete. The fluxional (broaden and temperature variant signals) material in **2** was assigned to **2tt** for three reasons. Conformer **2tt** was predicted to be fluxional by molecular mechanics. Pairs of pyridinium rings were

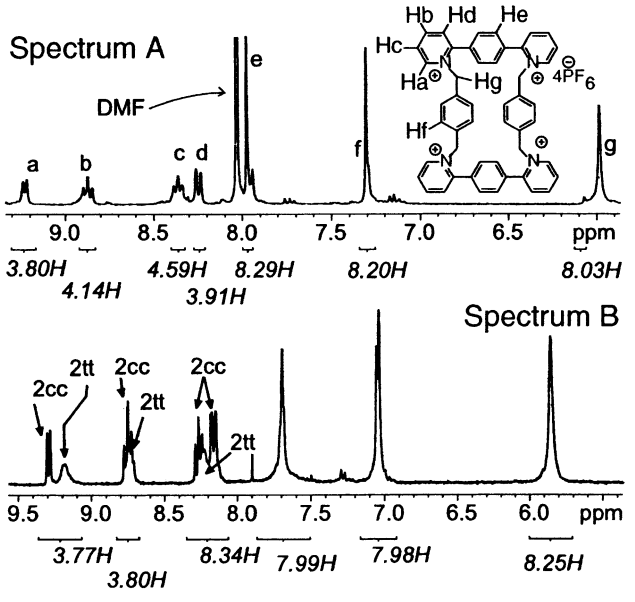

Figure 9. ^{1}H NMR spectra of **2**·4PF_6^- in DMF-d_4 Spectrum A and **2**·4Br^- in D_2O/MeOD-d_4 Spectrum B. The arrows indicate temperature and [NO_3^-]-sensitive features in the NMR spectrum assigned to conformer **2tt**. Note the absence of the fluxional component in **2** when dissolved in solvent of decrease dielectric constant.

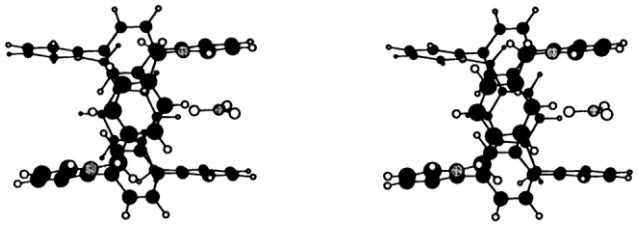

Figure 10. Stereodiagram of the calculated complex, **2tt**·NO_2^-. Nitrate anion bonded weakly between the proximal pyridine rings is visible to the right of the structure.

predicted to rest at unequal distances in **2tt** and the remote and proximal pair were predicted to exchange at low energy. These two pairs of pyridinium rings are evident upon examination of **2tt** in the stereodiagram in Fig. 4. Another reason for the assignment of the fluxional material in samples of **2** to **2tt** was the predicted and observed interaction of **2tt** with flat anions (sodium nitrate not bromide, chloride or sulfate). The transannular pairs of pyridinium rings in **2tt** should have served as molecular tweezers for these flat anions. The concept of molecular tweezers has been demonstrated.[24] Furthermore, calculations involving **2tt** and nitrate (all force fields/GBSA water) produced a stable complex with nitrate sandwiched between the transannular proximal pair of pyridinium rings in **2tt** (see Fig. 10). This interaction was borne out experimentally by weak binding constants ($\sim$80 M^{-1} in DMSO) in titrations of samples of **2**·$4Br^-$ and nitrate in D_2O/DMSO-d_6. The chemical shifts of the temperature-invariant component in **2**·$4Br^-$ (**2cc**) were not perturbed by these anions. The last reason for the assignment of the broad features in the ^1H NMR spectra of **2**·$4Br^-$ to **2tt** was the absence of these peaks when Br^- was exchanged for PF_6^- and the new salt was dissolved in organic NMR solvent (DMF). Compare the relevant spectra in the supplemental section. Conformer **2tt** should have been less stable in solvent of decreased polarity than **2cc** because solvent of high dielectric constant would have been needed to screen the proximal pyridinium rings in **2tt**; **2cc** bore remote transannular pyridinium rings and should have been relatively stable in organic solvent.

5. Conclusions

Macrocyclization to cyclophane derivatives **2** and **3** was most probably driven by π-stacking interactions and does not appear to have been impeded by electrostatic repulsion. Computation indicated that these cyclophanes were large enough to collapse and bring the neutral aromatic rings close enough to strongly interact. Low-energy conformers computed for cyclophanes **2** and **3** shared conformational motifs present in solid state derivatives of non-cyclophane **1a**–**g**. The barrier to exchange between **tt** and **cc** conformers was higher than predicted from molecular mechanics or from precedent of uncharged, analogous cyclophanes.

6. Experimental

6.1. General

All reactions were carried out under an atmosphere of nitrogen. Reagents were obtained commercially and used without further purification. DMF used as a solvent in all reactions was predried and distilled over calcium hydride and stored over 4-Å molecular sieves under nitrogen. Diethyl ether was pre-dried over Calcium chloride and distilled from sodium. NMR spectra were recorded on 200, 300 or 400 MHz spectrometers.

6.1.1. [1.1.1.1](*N*,*N′*,*N″*,*N‴*)*para*-2,2″-azaterphenylparacyclophanium (bromide and hexafluorophosphate salts), 2. *p*-2,2″-Diazaterphenyl (201 mg, 0.86 mmol) and 1,4-xylyl dibromide (229 mg, 0.86 mmol, 1 equiv.) were dissolved in dry DMF (2 mL) with heating in a nitrogen-purged flask and the reaction allowed to stir at 80°C for 24 h. The reaction was cooled to room temperature and DMF was removed by high vacuum rotary evaporation. Compound **2**·$4Br^-$ precipitated from methanol. Cyclophane **2** was more stable as the PF_6^- salt. Decomp. >257°C. ^1H NMR (300 MHz, CD_3OD) δ 5.86 (bs, 8H), 7.05 (bs, 8H), 7.69 (bs, 8H), 8.23 (m, 8H), 8.75 (td, 4H, J=7.9, 1.9 Hz), 9.19 (bs, 2H), 9.30 (d, 2H, J=6.4 Hz); ^{13}C NMR (PF_6^- salt, 100 MHz, DMF-d_4) δ 63.4, 129.5, 130.6, 131.5, 132.8, 135.7, 135.8, 136.1, 148.0, 148.2, 148.3, 148.5, 156.0. Anal. Calcd for $C_{48}H_{40}N_2(PF_6)_4$: C, 46.02; H, 3.22; N, 4.47. Found C, 46.08; H, 3.32; N, 4.31. FAB MS low res. *m*/*z* calcd 912.6 found. 912.7 $[M^{4+}+3Br^-]^+$, calcd 416.3 found 415.1 $[M^{4+}+2Br^-]^2+$.

6.2. General procedure for Br^-/PF_6^- exchange of 2 and 3[22]

To a solution of **2**·$4Br^-$ (100 mg) in water (1 mL) was added a saturated aqueous solution of NH_4PF_6. A white solid precipitated and was filtered and washed several times with ethanol to give the PF_6^- salt in quantitative yield.

6.2.1. [1.1.1.1](*N*,*N′*,*N″*,*N‴*)*para*-2,2″-Azaterphenylmetacyclophanium (bromide and hexafluorophosphate salts), 3. *p*-2,2″-Diazaterphenyl (201 mg, 0.86 mmol) and 1,3-xylyl dibromide (229 mg, 0.86 mmol) were dissolved in dry DMF (2 mL) with heating in a nitrogen purged flask at 75–80°C stirred for 24 h. The DMF was removed on a rotary evaporator, the solid residue was dried in vacuo and was recrystallized from methanol (0.353 g, 83%). Mp 244°C (decomp.) ^1H NMR (400 MHz, CD_3OD) δ 5.88 (bs, 8H), 7.07 (d, 4H, J=8.0 Hz), 7.20 (s, 2H), 7.23 (t, 4H, J=8.0 Hz), 7.75 (s, 8H), 8.2–8.4 (m, 8H), 8.75 (t, 4H, J=8.2 Hz), 9.16 (s, 4H); ^{13}C NMR (75 MHz, CD_3OD) δ 63.0 129.4, 129.8, 130.6, 131.5, 132.7, 135.6, 135.7, 135.8, 135.9, 147.8, 148.1, 155.9; Anal. Calcd for $C_{48}H_{40}N_4Br_4.H_2O$: C, 57.05; H, 4.18; N, 5.54; Found: C, 57.02; H, 4.27; N, 5.62. Anal. Calcd for $C_{48}H_{40}N_4(PF_6)_4$: C, 46.02; H, 3.22; N, 4.47; Found: C, 45.88; H, 3.16; N, 4.60.

6.2.2. 2,2″-*N*,*N′*-*para*-Diazaterphenyl, 4.[17] 2-Bromopyridine (24.5 g, 0.155 mol) was taken up in dry diethyl ether (400 mL) under N_2 at −78°C and treated with 1 equiv. *n*-butyl lithium (1.6 M solution in hexanes, 0.155 mol). The solution was stirred for 30 min at −78°C. Trimethyl borate (32.2 g, 0.31 mol, 2 equiv.) was added slowly over 90 min with stirring and the reaction mixture was allowed to warm to room temperature overnight. After evaporation of solvent, light impurities were removed via

azeotrope with dry MeOH (this step is crucial). A red–orange solid solidified under high vacuum. The yield of dimethyl pyridin-2-boronate was quantitative (as determined by ^{1}H NMR) and the material was used without further purification.

1,4-dibromobenzene (1.0 g, 4.34 mmol) was dissolved in dry dimethoxyethane (5 mL) in a flask fitted with a condenser. Tetrakis(triphenylphosphine)palladium (350.7 mg, 0.303 mmol, 0.07 equiv.) was added and the mixture allowed to stir at room temperature for 40 min. Dimethylpyridin-2-boronate (3.3 g, 21.7 mmol, 5 equiv.) in dry dimethoxyethane (15 mL) was added followed by the addition of crushed potassium hydroxide (1.2 g, 21.7 mmol, 5 equiv.). The reaction was allowed to reflux for 20 h. The reaction vessel was cooled to room temperature and water (20 mL) was added. The aqueous layer was extracted with EtOAc (4×15 mL) and the EtOAc phase was dried over $K_2CO_{3(s)}$. GC/MS analysis of the crude reaction mixture indicated 85% conversion. The organic residue was purified by flash silica chromatography, (hexane/ether/EtOAc, 5:4:2); material isolated from column chromatography was further purified by recrystallization from hexanes/ether (7:3) to yield 645 mg (64%) MP 138–140°C. ^{1}H NMR (400 MHz, $CDCl_3$) 7.98 (ddd, 2H, J=7.7, 5.7, 1.2 Hz), 8.13 (s, 4H), 8.33 (ddd, 2H, J=8.2, 1.2, 0.8 Hz), 8.58 (ddd, 2H, J=7.7, 8.2, 1.6 Hz), 8.80 (ddd, 2H, J=5.7, 1.6, 0.8 Hz); ^{13}C NMR (75 MHz, CDCl3) δ 64.4, 129.8, 130.0, 131.0, 131.4, 131.8, 132.5, 133.7, 133.9, 136.4, 148.6, 149.2, 158.4.

6.2.3. 2,2″-*N*,*N*′-*meta*-Diazaterphenyl, 5.[18] The method above was applied successfully to the *meta* derivative **5** only with the inclusion of 1 equiv. CuI after addition of the palladium catalyst. CuI supposedly competed with an inactive complex composed of **5** and the Pd catalyst. A viscous lt. yellow oil. ^{1}H NMR (400 MHz, $CDCl_3$, first order coupling analysis) 7.27 (ddd, 2H, J=7.3, 4.9, 1.3 Hz), 7.60 (td, 1H, J=7.7, 0.4 Hz), 7.79 (ddd, 2H, J=8.0, 7.3, 1.8 Hz), 7.86 (ddd, 2H, J=8.0, 1.3, 1.1 Hz), 8.07 (dd, 2H, J=7.7, 1.8 Hz), 8.64 (td, 1H, J=1.8, 0.4 Hz), 8.73 (ddd, 2H, J=4.9, 1.8, 1.1 Hz).

Acknowledgements

NSF CHE-9702287 supported this work. The 400 MHz NMR instruments used in this research were upgraded with funds from the CRIF program of the National Science Foundation (CHE 997841) and from the Research Challenge Trust Fund of the University of Kentucky. AC-G thanks R. L. Cerny, Ph.D. at the Nebraska Center for ESI and FAB MS analysis of **2**·4Br.

References

1. Martin, C. B.; Mulla, H. R.; Willis, P. G.; Cammers-Goodwin, A. *J. Org. Chem.* **1999**, *64*, 7802–7806.
2. Martin, C. B.; Patrick, B. O.; Cammers-Goodwin, A. *J. Org. Chem.* **1999**, *64*, 7807–7812.
3. Mulla, H. R.; Cammers-Goodwin, A. *J. Am. Chem. Soc.* **2000**, *122*, 738–739.
4. Sindkhedkar, M. D.; Mulla, H. R.; Cammers-Goodwin, A. *J. Am. Chem. Soc.* **2000**, *122*, 9271–9277.
5. For the nomenclature of these compounds see: Vögtle, F.; Neumann, P. *Tetrahedron* **1970**, *26*, 5847–5863.
6. Schladetzky, K. D.; Haque, T. S.; Gellman, S. H. *J. Org. Chem.* **1995**, *60*, 4108–4113.
7. For a similar argument regarding macrocyclization see: Pattarawarapan, S. R. M.; Roy, S.; Burgess, K. *Tetrahedron* **2000**, *56*, 9809–9818.
8. Ercolani, G.; Mandolini, L.; Masci, B. *J. Am. Chem. Soc.* **1981**, *103*, 2780.
9. Mandolini, L.; Masci, B. *J. Am. Chem. Soc.* **1977**, *99*, 7709.
10. Chapman, R. G.; Chopra, N.; Cochien, E. D.; Serman, J. C. *J. Am. Chem. Soc.* **1994**, *116*, 369–370.
11. Cram, D. J.; Karbach, S.; Kim, H. Y.; Baczynskyj, L.; Kalleymeyn, G. W. *J. Am. Chem. Soc.* **1985**, *107*, 2575–2576.
12. Chambron, J.-C.; Dietrich-Buchecker, C.; Sauvage, J.-P. In *Large Ring Molecules*; Semlyen, J. A., Ed.; Wiley: New York, 1996; pp 153–189.
13. Ashton, P. R.; Baldoni, V.; Balzani, V.; Claessens, C. G.; Credi, A.; Hoffmann, H. D. A.; Raymo, F. M.; Stoddart, J. F.; Venturi, M.; White, A. J. P.; Williams, D. J. *Eur. J. Org. Chem.* **2000**, 1121–1130.
14. Li, Z.-T.; Ji, G.-Z.; Zhao, C.-X.; Yuan, S.-D.; Ding, H.; Huang, C.; Du, A.-L.; Wei, M. *J. Org. Chem.* **1999**, *64*, 3572–3584.
15. *Large Ring Molecules*, Semlyen, J. A., Ed.; Wiley: New York, 1996.
16. Diederich, F. *Cyclophanes*, Vol. 2; Royal Society of Chemistry: Cambridge, UK, 1991.
17. Beley, M.; Collin, J.-P.; Louis, R.; Metz, B.; Sauvage, J.-P. *J. Am. Chem. Soc.* **1991**, *113*, 8521–8522.
18. Wiley, R. H.; Callahan, P. X.; Jarboe, C. H.; Nielsen, J. T. J.; Wakefield, B. J. *J. Org. Chem.* **1960**, *25*, 366–371.
19. Smithrude, D. B.; Sanford, E. M.; Chao, I.; Ferguson, S. B.; Carcanague, D. R.; Evanseck, J. D.; Houk, K. N.; Diederich, F. *Pure and Appl. Chem.* **1990**, *62*, 2227–2236.
20. Mohamadi, F.; Richards, N. G. J.; Guida, W. C.; Liskamp, R.; Lipton, M.; Caufield, C.; Chang, G.; Hendrickson, T.; Still, W. C. *J. Comp. Chem.* **1990**, *11*, 440.
21. Still, W. C.; Tempczyk, A.; Hawley, R. C.; Hendrickson, T. *J. Am. Chem. Soc.* **1990**, *112*, 6127–6129.
22. Lorente, A.; Fernandez-Saiz, M.; Herraiz, F.; Lehn, J. M.; Vigneron, J. P. *Tetrahedron Lett.* **1999**, *40*, 5901–5904.
23. Böckmann, K.; Vögtle, F. *Liebigs Ann. Chem.* **1981**, 467–475.
24. Zimmerman, S. C. *Top. Curr. Chem.* **1993**, *165*, 71–102.